Enhancement of high-temperature thermoelectric performances of $Bi_2Ba_2Co_2O_x$ ceramics

G. Constantinescu[a], Sh. Rasekh[a], M. A. Torres[b], M. A. Madre[a], J. C. Diez[a], A. Sotelo[a]

[a] Instituto de Ciencia de Materiales de Aragón (CSIC-Universidad de Zaragoza), Mª de Luna, 3. 50018 Zaragoza, Spain.
[b] Departamento de Ingeniería de Diseño y Fabricación, Universidad de Zaragoza, Mª de Luna, 3. 50018 Zaragoza, Spain.

Abstract

$Bi_2Ba_2Co_2O_x$ thermoelectric ceramics were textured from the melt using the laser floating zone method, at 5mm/h growth rate. Microstructure has shown a good grain alignment with the growth axis. These microstructural features have been reflected on the thermoelectric performances, with a very important increase on the power factor values, reaching ~0.4mW/K^2.m at 650ºC, much higher than the typical values obtained in this materials so far.

Keywords: Directional solidification, Electrical resistivity, Electroceramics, Thermoelectric materials, Cobaltites

Corresponding author: A. Sotelo. E-mail: asotelo@unizar.es. Tel.: +34 976762617; Fax: +34 976761957

Nowadays, thermoelectric (TE) power generation is considered as promising technology to harvest energy from different heat sources. As a consequence, it can be very useful in order to reduce CO_2 emissions in energy generation, helping to the global warming solution. For these applications, TE materials with high-energy conversion efficiency are strongly required for commercial devices. The performances of these materials are quantified by the dimensionless figure of merit, ZT, defined as $TS^2/\rho\kappa$ (where S is the Seebeck coefficient, T the absolute temperature, ρ the electrical resistivity and κ the thermal conductivity). From this definition, a high performance TE material should possess high Seebeck coefficient, with low electrical resistivity and thermal conductivity [1].

For the past two decades, intermetallic materials with high ZT have been widely applied in various sectors, e.g. automobile industry. Nonetheless, these materials have some drawbacks as their low stability at high temperature, which can result in degradation, oxidation, and/or evaporation. This situation has changed in 1997, by the discovery of large TE properties in the Na_xCoO_2 ceramic material [2]. Since then, great efforts have been performed to explore new TE materials, especially in the CoO-based families, with high TE performances. These works led to the discovery of new layered cobaltites, such as $[Ca_2CoO_3][CoO_2]_{1.62}$, $[Bi_{0.87}SrO_2]_2[CoO_2]_{1.82}$, and $[Bi_2Ba_2O_4][CoO_2]_{1.98}$ with promising TE properties [3-7].

The cobaltites crystal structure is formed by two different layers, which can be described as an alternate stacking of a common conductive CdI_2-type CoO_2 layer with a two-dimensional triangular lattice, and a block layer, composed of insulating rock-salt-type (RS) layers. These two sublattices possess common a- and c-axis lattice parameters and β angles while having different b-axis length, causing a misfit along the b-direction [7-10]. As a consequence, layered cobaltites possess a very high crystallographical anisotropy which, in turn, produces a high electrical one. For this reason, the alignment of their plate-like grains is essential to attain macroscopic properties comparable to those obtained on single crystals. Some methods have been shown to be adequate to obtain a good grain orientation in oxide ceramics, as template grain growth (TGG) [11], sinter forging [12], spark plasma sintering [13], or directional growth from the melt [14].

All texturing techniques, when applied in optimal conditions, produce well oriented grains which lead to the decrease on the electrical resistivity in the texturing direction. Among these techniques, the laser floating zone (LFZ) method has shown a high reliability to obtain good grain orientation in thermoelectric ceramic systems [14]. As a consequence, the samples grown by this technique show a reduction of electrical resistivity due to the good grain orientation and sizes [15]. On the other hand, previous studies on laser grown samples have shown that the textured samples produced by this technique possess higher Seebeck coefficient values than usual in these systems [16]. The aim of the present work is studying the TE performances of $Bi_2Ba_2Co_2O_x$ textured ceramics adequately prepared by the LFZ technique.

$Bi_2Ba_2Co_2O_x$ polycrystalline samples were prepared using the classical solid-state route from commercial Bi_2O_3 (Panreac, 98+%), $BaCO_3$ (Panreac, 99+%), and Co_2O_3 (Aldrich, 98+%) powders. They were weighed in the appropriate proportions, mixed and ball milled in acetone media at 300rpm for 30 minutes to produce a homogeneous mixture. The obtained powders suspension was then dried in a fast IR evaporation system. The remaining powder was manually ground and thermally treated twice, under air, at 750 and 800ºC for about 12 hours, with an intermediate manual milling. The objective of this process is assuring the barium carbonate decomposition, otherwise it would decompose in the molten zone, producing CO_2 bubbles inside the melt in the LFZ process, leading to the solidification front destabilization. The thermally treated powders were then milled, introduced into a latex tube (inner diameter ~3mm), and isostatically cold pressed at 200MPa for one minute to obtain green ceramic cylinders (~100mm long). The resulting cylinders were subsequently used as feed in a LFZ device equipped with a continuous power Nd:YAG laser (λ=1.06µm) which is described elsewhere [17].

All the LFZ grown samples were processed at 5mm/h under air, with a seed rotation of 3rpm anticlockwise while the feed was rotated at 15rpm, in the opposite direction, in order to assure the molten zone compositional homogeneity. After the texturing process, long (more than 150mm) and geometrically homogeneous (~2mm diameter) textured cylindrical rods have been produced. Finally, the textured bars were cut into pieces with the adequate dimensions for their characterization (~15mm long pieces).

The identification of the main phases in textured samples has been carried out using powder XRD in a Rigaku D/max-B X-ray powder diffractometer (CuKα radiation), between 10 and 40 degrees. X-ray line broadening measurements have been used in order to estimate the plate-like grain thickness, according to Scherrer formula [18]. Microstructures have been observed using a scanning electron microscope (SEM, JEOL 6000) equipped with an energy X-ray dispersive spectroscopy (EDS) system. Longitudinal polished sections of textured samples have been observed to evaluate the spatial phases distribution. Different contrasts have been studied by EDS to qualitatively determine their composition. Image analysis has been performed on several micrographs in order to estimate the volume fraction of each phase. Electrical resistivity and Seebeck coefficient have been simultaneously determined by the standard dc four-probe technique in a LSR3 measurement system (Linseis GmbH) under He atmosphere, in the steady state mode, at temperatures ranging from 50 (~room temperature) to 650°C. Samples performances have been determined with the power factor (PF=S^2/ρ), calculated from the measured electrical resistivity and Seebeck coefficient data.

Powder XRD patterns for the $Bi_2Ba_2Co_2O_x$ textured samples are displayed in Fig. 1. From that pattern, three main phases have been identified: $Bi_2Ba_2Co_2O_x$, $BiBaO_3$ and $Ba_5Co_5O_{14}$. The peaks corresponding to the cobaltite phase have been indexed and are in agreement with previously reported data [19]. The peak marked by a $\star$ corresponds to the $BiBaO_3$ secondary phase with P121/n1 space group [20] and those indicated by a $\triangledown$ are associated to the $Ba_5Co_5O_{14}$ one with $P\bar{3}m1$ space group [21].

SEM micrographs performed on fractured longitudinal sections of the samples have shown that samples are composed of well oriented plate-like grains which can easily reach 500μm length in the a or b directions (see insert in Fig. 2). On the other hand, their thickness is difficult to measure as these plate-like grains are, in turn, formed by many thin grains well stacked along the ab planes. In order to overcome this problem, the individual plate-like grain thickness has been estimated from the X-ray line broadening measurements using the (0030) and (0060) diffraction lines of the $Bi_2Ba_2Co_2O_x$ phase, according to the Scherrer formula [18]. The obtained mean value for the grain thickness is around 45nm which clearly indicates that the crystal

preferential growth is produced along the ab plain (coincident with the conducting CoO planes).

A representative SEM micrograph, performed on a polished longitudinal section of the textured samples is displayed in Fig. 2. The different phases in the samples have been associated, through EDS, with the different contrasts found in the micrographs, and numbers in Fig. 2. Grey contrast (#1) corresponds to the major phase (~80vol.%) and it has been identified as the thermoelectric $Bi_2Ba_2Co_2O_x$ one. Dark grey contrast (#2, ~8vol.%) corresponds to the $Ba_5Co_5O_{14}$ phase, appearing as long and thin grains which show a relatively good alignment with the growth direction. White contrast (#3, ~11vol.%), with $BiBaO_3$ composition, appears as thicker and shorter grains than the $Ba_2Co_3O_y$ phase, between the thermoelectric grains. Finally, black contrasts (#4, <0.5vol.%) has been identified as CoO and it is the only phase not detected in XRD, due to its low amount. Other interesting feature observed in Fig. 2 is the very big length of the thermoelectric phase grains (in agreement with the fracture observations described previously) which assure a good electrical continuity all along the samples in the growth direction. The size of thermoelectric grains can be explained by the high stability of the LFZ growth system which, at the selected growth conditions (growth rate, laser power, rotation, ...), provides a very stable solidification front.

In order to study the effect of texturing on the thermoelectric properties of $Bi_2Ba_2Co_2O_x$ samples, the temperature dependence of the electrical resistivity has been measured and represented in Fig. 3. In this figure it can be clearly seen that samples possess a slight metallic-like behaviour from room temperature to ~200ºC, where resistivity values increase with temperature from ~10.0 to ~10.5mΩ.cm. At higher temperatures, samples show semiconducting-like behaviour and measured resistivity decreases to a minimum of ~8.5mΩ.cm (at 650ºC), which is around the best reported values for this kind of materials at the same temperature (~6mΩ.cm) [22].

In Fig. 3 it is also presented the Seebeck coefficient variation with temperature for the $Bi_2Ba_2Co_2O_x$ textured samples. S values are positive in all the measured temperature range, indicating a predominating hole-conduction mechanism. Measured S values on LFZ grown samples at room temperature (about 120μV/K) are higher than best reported ones for this material at the same temperature, around 90μV/K [22]. Moreover, they

increase quasilinearly with temperature from about 120μV/K, at room temperature, to about 170μV/K at 450ºC. At higher temperatures, also a nearly linear increase with temperature is produced, but with a lower slope. This raise in S values with temperature is higher than the best reported samples in this system which allow reaching improvements of about 170% at 650ºC with respect to the best reported values at the same temperature (around 110 μV/K) [22]. The explanation of the high S values obtained in the $Bi_2Ba_2Co_2O_x$ textured samples, with respect to those obtained on samples prepared using conventional routes, is due to the formation of considerable amounts of oxygen vacancies on the thermoelectric phase when samples are processed using the LFZ technique [23,24]. This effect has also been observed in the misfit $[Ca_2CoO_3][CoO_2]_{1.62}$ phase which contains considerable amounts of oxygen vacancies when it is thermally treated under reducing atmosphere [25]. The raise on the oxygen vacancies partially change the Co oxidation state from Co^{4+} to Co^{3+} and, as a consequence, S values increase, in agreement with Koshibae equation [26].

In order to evaluate the thermoelectric performances of textured $Bi_2Ba_2Co_2O_x$ ceramic materials, variation of PF with temperature has been calculated from the resistivity and Seebeck coefficient values, and displayed in Fig. 4. In this figure it can be clearly seen that PF increases following a parallel behaviour to that observed in the S values. This is due to the very small variation of resistivity with temperature. Moreover, the highest PF value obtained at 650ºC (~0.4mW/K^2.m), is about 10 times higher than the best previously reported values for this composition at the same temperature (0.04mW/K^2.m at 650ºC) [22], making this material a promising one for practical applications.

In summary, this work demonstrates that $Bi_2Ba_2Co_2O_X$ thermoelectric ceramics can be successfully grown using the laser floating zone (LFZ) technique. The textured samples are formed by large grains (more that 500μm in the ab plane) which are very well aligned with respect to the growth axis. These microstructural features lead to a relatively low electrical resistivity values and high Seebeck coefficient. The highest power factor value obtained at 650ºC for the LFZ grown samples, around 0.4mW/K^2m, is about 10 times higher than the best reported values for this composition making this textured material a promising candidate for practical applications in the next power generation systems.

References

[1] Rowe DM. In: Rowe DM, editor. Thermoelectrics handbook: macro to nano. 1st ed. Boca Raton, FL: CRC Press; 2006. p. 1-3.

[2] I. Terasaki, Y. Sasago, and K. Uchinokura, Phys. Rev. B 56 (1997) 12685.

[3] R. Funahashi, I. Matsubara, H. Ikuta, T. Takeuchi, U. Mizutani, S. Sodeoka, Jpn. J. Appl. Phys. 39 (2000) L1127.

[4] A. C. Masset, C. Michel, A. Maignan, M. Hervieu, O. Toulemonde, F. Studer, B. Raveau, J. Hejtmanek, Phys. Rev. B 62 (2000) 166.

[5] H. Leligny, D. Grebille, O. Perez, A. C. Masset, M. Hervieu, B. Raveau, Acta Crystal. B 56 (2000) 173.

[6] A. Maignan, D. Pelloquin, S. Hébert, Y. Klein, M. Hervieu, Bol. Soc. Esp. Ceram. V. 45 (2006) 122.

[7] W. Kobayashi, S. Hebert, H. Muguerra, D. Grebille, D. Pelloquin, A. Maignan, Thermoelectric properties in the misfit-layered-cobalt oxides $[Bi_2A_2O_4]$ $[CoO_2]_{b1/b2}$ (A=Ca, Sr, Ba, b(1)/b(2)=1.65, 1.82, 1.98) single crystals. In: I. Kim I (Ed.), Proceedings ICT 07: 26th international conference on thermoelectrics, IEEE, New York, 2008, pp. 117–20.

[8] A. Maignan, S. Hebert, M. Hervieu, C. Michel, D. Pelloquin, D. Khomskii, J. Phys.: Condens. Matter; 15 (2003) 2711.

[9] F. P. Zhang, Q. M. Lu, J. X. Zhang, J. Alloy. Compd. 484 (2009) 550.

[10] H. Itahara, C. Xia, J. Sugiyama, T. Tani, J. Mater. Chem. 14 (2004) 61.

[11] E. Guilmeau, M. Mikami, R. Funahashi, D. Chateigner, J. Mater. Res. 20 (2005) 1002.

[12] Y. Masuda, D. Nagahama, H. Itahara, T. Tani, W. S. Seo, K. Koumoto, J. Mater. Chem. 13 (2003) 1094.

[13] J. G. Noudem, D. Kenfaui, D. Chateigner, M. Gomina, J. Electronic Mater. 40 (2011) 1100.

[14] J. C. Diez, Sh. Rasekh, M. A. Madre, E. Guilmeau, S. Marinel, A. Sotelo, J. Electronic Mater. 39 (2010) 1601.

[15] A. Sotelo, E. Guilmeau, Sh. Rasekh, M. A. Madre, S. Marinel, J. C. Diez, J. Eur. Ceram. Soc. 30 (2010) 1815.

[16] A. Sotelo, Sh. Rasekh, E. Guilmeau, M. A. Madre, M. A. Torres, S. Marinel, J. C. Diez, Mater. Res. Bull. 46 (2011) 2537.

[17] G. F. de la Fuente, J. C. Diez, L. A. Angurel, J. I. Peña, A. Sotelo, R. Navarro, Adv. Mater. 7 (1995) 853.

[18] A. L. Patterson, Phys. Rev. 56 (1939) 978.

[19] H. Hao, H. Yang, Y. Liu, X. Hu, J. Mater. Sci. Technol. 27 (2011) 525.

[20] B. J. Kennedy, C. J. Howard, K. S. Knight, Zhang Zhao Ming, Zhou Qing Di, Acta Cryst. B 62 (2006) 537.

[21] K. Boulahya, M. Parras, J. M. Gonzalez-Calbet, U. Amador, J. L. Martinez, V. Tissen, M. T. Fernandez Diaz, Phys. Rev. B - Condens. Matter. 71 (2005) 144402.

[22] R. Ang, Y. P. Sun, X. Luo, W. H. Song, J. Appl. Phys. 102 (2007) 073721.

[23] J. C. Diez, E. Guilmeau, M. A. Madre, S. Marinel, S. Lemonnier, A. Sotelo, Solid State Ionics 180 (2009) 827.

[24] A. Sotelo, E. Guilmeau, M. A. Madre, S. Marinel, S. Lemmonier, J. C. Diez, Bol. Soc. Esp. Ceram. V. 47 (2008) 225.

[25] M. Karppinen, H. Fjellvåg, T. Konno, Y. Morita, T. Motohashi, H. Yamauchi, Chem. Mater. 16 (2004) 2790.

[26] W. Koshibae, K. Tsutsui, S. Maekawa, Phys. Rev. B 62 (2000) 6869.

Figure captions

Figure 1. Powder XRD plot of the $Bi_2Ba_2Co_2O_x$ textured specimens. The peaks corresponding to the $Bi_2Ba_2Co_2O_x$ thermoelectric phase are indexed while * indicates the $BiBaO_3$ secondary phase and $\triangledown$ the $Ba_5Co_5O_{14}$ one.

Figure 2. Scanning electron micrographs from longitudinal polished $Bi_2Ba_2Co_2O_x$ textured samples. The arrows indicate the different contrasts. #1, grey contrast thermoelectric $Bi_2Ba_2Co_2O_x$ phase; #2, dark grey ($Ba_5Co_5O_{14}$); #3, white ($BiBaO_3$); and #4 black one (CoO). Insert shows the good orientation of the plate-like grains.

Figure 3. Temperature dependence of the electrical resistivity and Seebeck coefficient for $Bi_2Ba_2Co_2O_x$ textured samples.

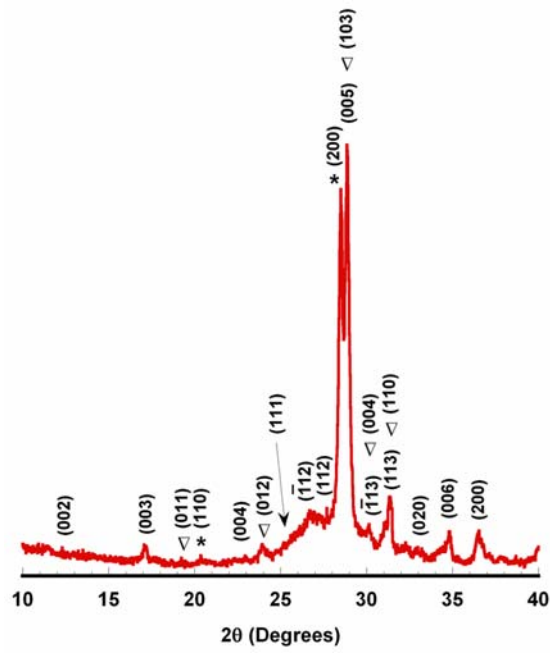Figure 4. Temperature dependence of the power factor for $Bi_2Ba_2Co_2O_x$ textured samples.
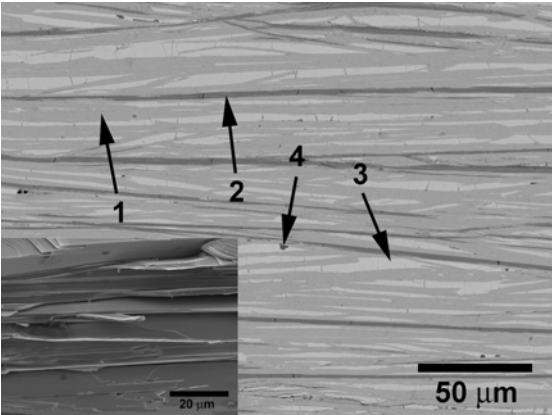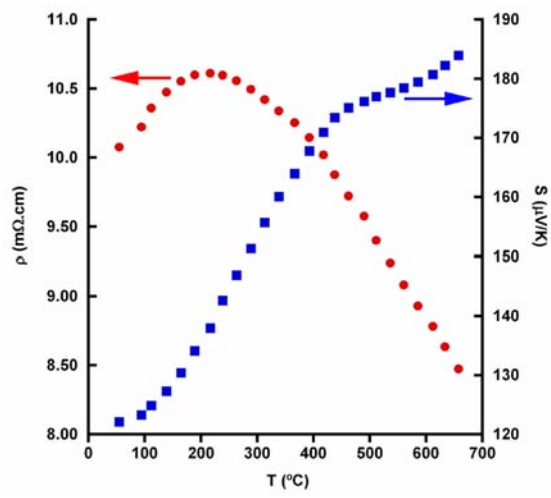
Figure 1

Figure 2

Figure 3

Figure 4